Acta Cryst. (1993). A49, 1-10

Benzene, Naphthalene and Anthracene Dimers and their Relation to the Observed Crystal Structures

BY DONALD E. WILLIAMS AND YONGLIANG XIAO

Department of Chemistry, University of Louisville, Louisville, KY 40292, *USA*

(*Received* 20 *February* 1992; *accepted* 18 *May* 1992)

Abstract

Molecular packing in benzene, naphthalene and anthracene crystals is analyzed in terms of molecular dimer interaction. Intermolecular energies of the gas dimer molecules are calculated for various intermolecular distances and orientations using empirical (exp − 6 − 1) potential-energy functions. The gas dimers are compared to pairs of molecules extracted from the observed crystal structures. Particular attention is given to intermolecular Coulombic interaction. Net atomic charges are obtained by the potential-derived method from 6-31*G* and 6-31*G*** level *ab initio* wavefunctions. In the benzene crystal there are strong edge-plane intermolecular Coulombic interactions. The edge-plane interaction becomes somewhat less important in naphthalene and anthracene and the van der Waals interaction increases in importance.

Introduction

Models for intermolecular interaction energies utilize levels of sophistication that are compromises between the needs for accuracy and mathematical simplicity. The simplest possible treatment is the atomic hard-sphere model, which defines a prohibited overlap region of space for each molecule; the remainder of configuration space is considered to be freely available. Crystal-structure studies confirm the usefulness of the concept of minimum cell volume subject to hard-sphere radii. However, there exist orientational effects in aromatic hydrocarbon crystals that cannot be explained with a hard-sphere model. A soft-sphere model, while an improvement, is still unsatisfactory.

At the next level of sophistication, a generally attractive energy must be added; otherwise molecules would never cluster together and liquify or crystallize. This is the omnipresent dispersion energy (the only attractive component for noble gases), which accounts for their condensation. For many organic molecules, particularly hydrocarbons, dispersion energy is also the major component of the attractive energy. According to theory, dispersion energy is related to polarizability and can be anisotropic. Early attempts to explain 'herringbone' crystal structures of aromatic hydrocarbons were often based on an anisotropic dispersion effect (Sternlicht, 1964).

It was then commonly thought that very little of the crystal energy of hydrocarbons was electrostatic in nature. The carbon-hydrogen bond was not believed to be highly polarized and the electric potential surrounding such molecules was thought to be negligible. Hydrocarbons epitomized 'hydrophobic interaction' with a near-total lack of electrostatic interaction. However, crystal-structure studies of aromatic hydrocarbons (Williams, 1974) showed substantial electrostatic energy. Williams & Starr (1977) found net atomic charges of 0.153e on the hydrogen atoms of benzene; the charge was found necessary to model benzene crystal structures at low and high pressures (Hall & Williams, 1975; Hall, Starr, Williams & Wood, 1980). Furthermore, the existence of these small but significant atomic charges gave a different but reasonable explanation of herringbone packing patterns almost uniformly observed in aromatic hydrocarbons (Gavezzotti, 1989). In this view, herringbone packing results from positively charged hydrogens on the edge of a molecule being attracted by Coulombic force to negatively charged ring carbons of adjacent molecules, favoring an edge-plane orientation of molecular dimers.

In favorable cases of high symmetry, net atomic charges can be obtained from molecular electric moments. For instance, charges on the atoms of the benzene molecule can be set from the observed quadrupole moment. These charges agree quite closely with the charge mentioned above derived from crystal structures. However, the electric moments of less-symmetrical molecules provide insufficient detail. In naphthalene, it is well established that the α and β positions have very different reactivity and therefore probably have different net atomic charges. The actual charges can be estimated from the wavefunction of the molecule calculated by *ab initio* quantum mechanics.

For van der Waals complexes of small polar molecules, the observed orientation of molecules can often be predicted from electrostatic interaction alone or in conjunction with hard-sphere atoms. Liu & Dykstra (1986) examined electrostatic influence on molecular orientation in over 20 hydrogen-bonded and other weakly bonded complexes of small molecules. They concluded that the electrostatic model for orientation was successful in every case,

0108-7673/93/010001-10$06.00

except possibly the ammonia dimer. Buckingham & Fowler (1983, 1985) also argue that electrostatic interaction and hard-sphere repulsion is sufficient to predict the structure of van der Waals complexes of small molecules. In a later paper, Hurst, Fowler, Stone & Buckingham (1986) concede that although, in general, electrostatic interaction is central to the strength and orientation dependence of van der Waals complexes, it is not a complete picture. Price & Stone (1987) studied electrostatic interactions in van der Waals complexes involving aromatic molecules. Benzene dimer and clusters (Steed, Dixon, & Klemperer, 1979; van de Waal, 1984; Carsky, Selzle & Schlag, 1988; Valente & Bartell, 1984; Bartell, Harsanyi & Valente, 1989) have been the subject of much interest, where it is known that observed noncoplanar arrangements of benzene molecules cannot be predicted with a simple no-charge van der Waals interaction model. Shi & Bartell (1988) investigated the transition from coplanar packing to the observed herringbone packing in crystalline benzene. They determined that an atomic charge of at least 0.09e on hydrogen was necessary to predict the observed crystal structure. Hall, Starr, Williams & Wood (1980) also found that the transition of orthorhombic benzene (atmospheric pressure) to monoclinic (25×10^8 Pa pressure) could not be modeled unless atomic-charge interactions were included.

Similar approaches have been taken for interactions between biomolecules. Warshel (1981) proposed that the single most important element in structure-function correlation in protein interaction (*e.g.* enzyme catalysis) was the electrostatic energy. Similar conclusions were drawn by Hwang & Warshel (1987), Politzer, Laurence & Jayasuriya (1985) and Venanzi & Bunce (1986). In a review of the molecular mechanics and dynamics of proteins, Kollman & van Gunsteren (1987) note that proteins are relatively unstrained molecules and thus the most critical parameters in a protein force field are the nonbonded ones, *i.e.* van der Waals and electrostatic. The great importance of electrostatic interaction between organic and bio-organic molecules is thus well established, although not to the exclusion of other effects. In the following sections, the number of significant figures given for net atomic charges or derived energies is intended to allow reproduction of the results and is not intended to portray their accuracy. The question of accuracy is a difficult one; it is addressed to some extent in the discussions.

Comparison of net-atomic-charge models

Wave functions for benzene, naphthalene and anthracene molecules were calculated by the *ab initio* self-consistent-field (SCF) molecular-orbital method. As a compromise between demands for accuracy and minimizing the computer time required, the 6-31G** Gaussian basis set was selected for the benzene and naphthalene molecules and 6-31G for the anthracene molecule. The geometry of benzene is the same as one selected by Williams (1980) for comparison to the previous work. Neutron diffraction crystal-structure data were used for naphthalene (Natkaniec, Belushkin, Dyck, Fuess & Zeyen, 1983) and anthracene (Chaplot, Lehner & Pawley, 1982) so as to get more accurate geometries for hydrogen positions. The molecular electrostatic potential was calculated for each molecule and the Mulliken charges were calculated in each case for the purpose of comparison with potential-derived (PD) charges (Cox & Williams, 1981). The program *GAUSSIAN*86 (Frisch *et al.*, 1988) was used with a VAX computer.

Table 1. *Mulliken and PD charges (in absolute electron units) for benzene, naphthalene and anthracene*

	Atoms	Mulliken charge	PD charge*
Benzene	C	−0.1872	−0.1464
	H	0.1872	0.1464
Naphthalene	Cα	−0.1336	−0.3592
	Hα	0.1535	0.1991
	Cβ	−0.1580	−0.1402
	Hβ	0.1514	0.1617
	C	−0.0266	0.2772
Anthracene	Cα	−0.1748	−0.6022
	Hα	0.2210	0.2658
	Cβ	−0.1624	−0.3108
	Hβ	0.2098	0.1895
	Cγ	−0.2117	−0.1653
	Hγ	0.2032	0.1715
	C	−0.0620	0.2833

* PD charges were calculated with hydrogen positions moved 0.07 Å toward the carbon position to be consistent with the force field, which used foreshortened carbon–hydrogen bonds.

The electric potential for a unit positive charge at a point **r** in the vicinity of the given molecule is given by

$$\mathbf{V}(\mathbf{r}) = \sum_A Z_A/|\mathbf{r}-\mathbf{R}_A| - \sum_{m,n} P_{mn} \int \Phi_m\Phi_n/|\mathbf{r}-\mathbf{r}'|\, d\mathbf{r}',$$

where P_{mn} is an element of the density matrix of the SCF molecular wave function and Φ_m are the basis functions used as a basis set. The first term is summed over the nuclei and the second term is summed over the electrons of the system.

The set of points selected for the evaluation of the electric potential was a cubic grid of 0.6 Å in a 1.2 Å thick van der Waals shell around the molecule, which generated about 1600 grid points for benzene, and about 2460 grid points for naphthalene and anthracene. This choice of grid was finer than many grids used successfully in the past (Williams, 1991*b*). Grid fineness was limited by the computer power available; larger computers can utilize even more finely spaced grids. The electric potential at each grid point was calculated directly from the *ab initio* wavefunction.

Table 2. *Comparison of different charge models for the molecular packing*

	Charge model	Theta shift*(°)	% change			$\Delta\beta$(°)	Total energy (kJ mol^{-1})
			a	*b*	*c*		
Benzene	No charge	21.8	−7.6	1.8	12.3	-	−43.03
	Mulliken charge	20.4	6.5	−15.5	16.4	-	−57.65
	PD charge	3.0	0.2	−0.8	4.6	-	−51.53
Naphthalene	No charge	3.7	−0.5	3.6	−3.1	−3.5	−69.91
	Mulliken charge	3.4	0.9	−2.8	2.1	−1.7	−96.61
	PD charge	1.5	0.6	0.3	0.9	−1.3	−79.05
Anthracene	No charge	5.1	0.0	5.3	−3.0	−1.6	−95.74
	Mulliken charge	5.5	2.2	−4.3	4.3	−0.4	−138.74
	PD charge	1.9	0.1	1.0	0.7	−1.3	−102.93

* Theta shift is the magnitude of the angle between observed and calculated molecular orientations.

The program *PDM*88 (Williams, 1988) was used to calculate PD charges and values are listed in Table 1. Calculated Mulliken charges for benzene were $q_C = -0.187$e and $q_H = 0.187$e, while the PD charges were $q_C = -0.146$e and $q_H = 0.146$e. The PD values are in good agreement with the Williams & Starr (1977) calculated value of $q_C = -0.153$e, and also with the observed quadrupole moment. There are large differences between Mulliken charges and PD charges in naphthalene and anthracene. There is even a change of sign in the charge of the ring-fusion carbon. Note that, in naphthalene, charges at the α and β positions are different and that the charge on the fusion carbon is not zero. A similar situation prevails in anthracene.

The model used for calculation of the intermolecular energy of the dimers is called (exp − 6 − 1), where the intermolecular energy is represented as an atom-atom sum of Coulombic interaction between net charges, dispersion attraction and exponential respulsion,

$$E = \mathrm{REP} + \mathrm{DISP} + \mathrm{COUL},$$

where

$$\mathrm{REP} = \tfrac{1}{2}\sum_j \sum_k B_{jk} \exp(-C_{jk} r_{jk}),$$

$$\mathrm{DISP} = \tfrac{1}{2}\sum_j \sum_k -A_{jk} r_{jk}^{-1},$$

$$\mathrm{COUL} = \tfrac{1}{2}\sum_j \sum_k q_j q_k r_{jk}^{-1}$$

and r_{jk} is the nonbonded distance between atoms j and k in different molecules. The first term, REP, in the intermolecular energy expression is the short-range repulsion energy. The second term, DISP, is the dispersion attraction energy. It is convenient to represent the sum of REP and DISP as the van der Waals energy, vdW. The third term, COUL, gives the interaction between net atomic charges. Values of A, B and C are taken from Williams & Starr (1977), where they were fitted to observed crystal structures. The net atomic charges are small but not negligible for hydrocarbons. To examine the structural effects of the COUL component, several models for net atomic charges were examined. These models were zero charge, Mulliken charge and PD charge.

In their study of experimentally determined hydrocarbon crystal structures, Williams & Starr (1977) assumed that the charge separation in a C–H bond was constant and that a carbon with no hydrogen (*e.g.* a ring-fusion carbon) has zero charge. They optimized the value of this charge-separation parameter for a series of 18 crystal structures of both aromatic and saturated molecules. This led to derived charges of $q_C = -0.153$e and $q_H = 0.153$e in C–H groups. The PD charge value of 0.1464e obtained independently by *ab initio* theoretical methods for benzene is very close to the value of 0.151e obtained from the observed quadrupole moment (Battaglia, Buckingham & Williams, 1981). As noted above, an advantage of the PD method is that a distinction is made between different types of C–H groups and a net charge can be obtained even for the ring-fusion carbons in naphthalene and anthracene without recourse to experimental multipole-moment values. Table 2 shows the results of minimizing the crystal energy of the three compounds using no-charge, Mulliken-charge and PD-charge models. Program *PCK*91 (Williams, 1991*a*) was used for the calculations.

Even for these relatively nonpolar hydrocarbons there are differences between crystal-energy calculations that include net atomic charges and those not including charges. If charges are included, their effect may create a negative total Coulombic energy that stabilizes the structures. This stabilizing effect is most important for benzene, where the Coulombic energy is 16% of the total energy. In naphthalene and anthracene the Coulombic energies decrease to 12 and 8% of the respective total energies.

In benzene, the Mulliken-charge model predicts a crystal structure which is actually worse than a no-charge model. In the case of naphthalene and anthracene, the Mulliken and no-charge models are equally poor. The predicted benzene crystal structure is particularly sensitive to values of atomic charges, as compared to naphthalene or anthracene. Shi & Bartell (1988) determined that a sharp deterioration in the quality of prediction of the benzene crystal

Table 3. *Coplanar, cross and edge models of aromatic molecule dimers*

	Model	Z translation (Å)	Slide translation	Slide (Å)	Center-to-center separation (Å)	vdW (kJ mol^{-1})	COUL (kJ mol^{-1})	Energy (kJ mol^{-1})
Benzene	Coplanar	3.70	None		3.70	−16.68	8.93	−7.75
	Slide	3.70	X	2.31	4.36	−12.34	2.52	−9.81
	Edge	5.10	None		5.10	−7.70	−2.36	−10.06
Naphthalene	Coplanar	3.70	None		3.70	−32.64	11.73	−20.89
	Slide	3.70	X	1.40	3.96	−29.81	7.91	−21.89
	Slide	3.70	Y	1.60	4.03	−30.24	6.70	−23.53
	Cross	3.60	None		3.60	−33.20	8.29	−24.09
	Slide	3.60	X	0.40	3.62	−33.00	8.07	−24.91
	Edge	5.20	None		5.20	−13.85	−4.79	−18.64
Anthracene	Coplanar	3.60	None		3.60	−50.46	16.34	−34.10
	Slide	3.60	X	1.40	3.86	−46.87	10.08	−36.77
	Slide	3.60	Y	1.60	3.94	−48.42	10.53	−37.86
	Cross	3.40	None		3.40	−46.19	1.85	−44.34
	Slide	3.40	X	0.00	3.40	−46.19	1.85	−44.34
	Edge	5.20	None		5.20	−21.46	−6.55	−28.01

structure occurred below an atomic charge of about 0.09. The Mulliken-charge entry in Table 2 indicates that the large Mulliken charge of 0.1872e also degrades the quality of the prediction of the benzene crystal. The PD charge values of 0.1464e does a much better job of predicting the observed crystal structure. For all three crystals, PD-charge models are superior to no-charge or Mulliken-charge models. Naphthalene and anthracene crystal structures are less sensitive to changes in the charge models; a rationale for this behavior is given later.

Gas dimer interaction energy

When finding the optimum structure of a molecular dimer, one molecule may be fixed to define the rotational and translational origin. The second molecule, if unconstrained, is allowed to freely rotate and translate with six degrees of freedom until an intermolecular-energy minimum is reached. For a better understanding of spatial relationships of molecules in the dimer, several constrained orientations were considered. The reference molecule was placed in the XY plane with its long axis along X. In the coplanar model, the second molecule is placed on top at a distance Z; in the cross model, the molecule on top is rotated 90° around an axis between the molecular centers; in the edge model, one molecule can be perpendicular to the other. In addition, the top molecule can be allowed to slide along X or Y. The intermolecular energy of these models was computed for different distances between molecular centers. The nonbonded parameters of Williams & Starr (1977) were used with the PD charges shown in Table 1. Table 3 specifies the minimum-energy structures obtained for the models, giving intermolecular center-to-center distances and calculated intermolecular energies. All calculations were made on a Vaxstation 3100 using program *PCK*91 (Williams, 1991*a*).

Benzene dimer

The coplanar, cross and edge models of the benzene dimer were studied with the intermolecular distance varied between 2.0 and 9.5 Å at intervals of 0.1 Å. There was no significant difference between the coplanar and cross models for the benzene dimer. Fig. 1 shows how the intermolecular energy changes with molecular center-to-center distance. The minimum energy of the coplanar model was −7.75 kJ mol^{-1} at a distance of 3.70 Å. Keeping the interplanar distance constant and sliding along either X or Y gave a minimum energy of −9.81 kJ mol^{-1} at a slide distance of 2.31 Å (Fig. 2). The edge model showed a lower energy of −10.06 at the greater distance of 5.10 Å.

It is clear that the edge model is best for benzene even though the distance between molecular centers is larger and therefore van der Waals stabilization is small. Table 3 shows that in going from the coplanar to the edge model, COUL decreases by 11.29 kJ mol^{-1} but vdW increases by only 8.98 kJ mol^{-1}. This gives a net additional stabilization of 2.31 kJ mol^{-1} for the edge model. Sliding the top molecule to eliminate

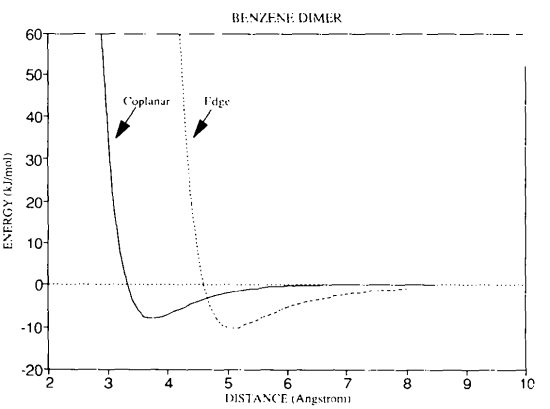

Fig. 1. Coplanar and edge models for benzene.

superposed identical atoms decreases COUL by 6.41 kJ mol^{-1} while 4.34 kJ mol^{-1} of vdW is lost. The net gain of 2.06 kJ mol^{-1} is only slightly less than was obtained in going to the edge model. Thus, the slide model is nearly as good as the edge model. Williams (1980) showed that, if all constraints are removed, the energy is −10.97 kJ mol^{-1} and the predicted structure is intermediate between the edge and slide models.

The results for the edge model are in fair agreement with *ab initio* theoretical calculations by Carsky, Selzle & Schlag (1988), who obtained an energy of −7.82 kJ mol^{-1} at a distance of 5.0 Å; their values include empirical estimates of dispersion energy. However, their calculations agree less well with the coplanar model, where they obtained an energy of −1.09 kJ mol^{-1} at a distance of 4.5 Å.

Naphthalene dimer

Results for naphthalene are shown in Fig. 3. The coplanar model has a minimum at the same distance as the coplanar model for benzene, 3.70 Å. As with benzene, COUL decreases when the top molecule is slid along *X* or *Y* (Fig. 4). The slide along *Y*, the long axis of the molecule, is most effective, where COUL decreases by 5.03 kJ mol^{-1} while vdW increases by only 2.40 kJ mol^{-1} to give a net lowering of 2.64 kJ mol^{-1} to the energy at a slide distance of 1.60 Å. In the cross model (Fig. 5), both vdW and COUL are lowered even more than in the coplanar model. A short slide of 0.40 Å in the cross model gives the lowest energy, −24.91 kJ mol^{-1}.

In contrast to benzene, the edge model is not favored because the drastic increase in vdW (+18.79 kJ mol^{-1} from the coplanar model) is not compensated by the decrease in COUL (−16.52 kJ mol^{-1}). The edge model is thus 2.25 kJ mol^{-1} higher in energy than the coplanar model. The calculations show that a strict edge orientation is not preferred in the naphthalene dimer. It is probable, however, that, as in benzene, an intermediate model with a structure between the edge and coplanar models will be optimum.

Anthracene dimer

The anthracene dimer behaves basically in the same way as naphthalene dimer, but the coplanar

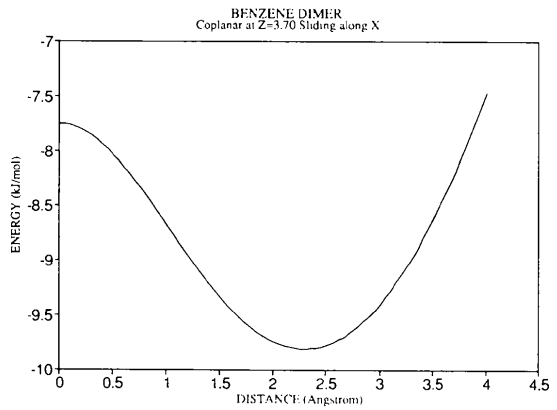

Fig. 2. Sliding model for benzene.

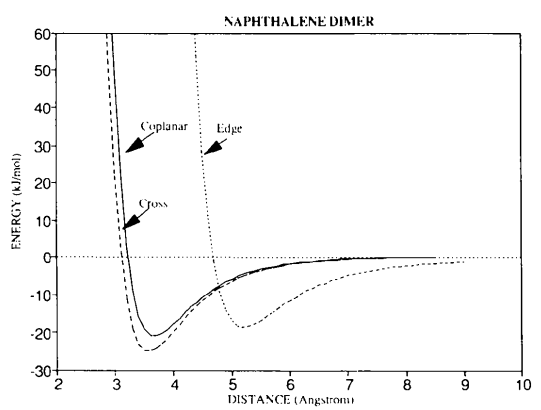

Fig. 3. Coplanar, cross and edge models for naphthalene.

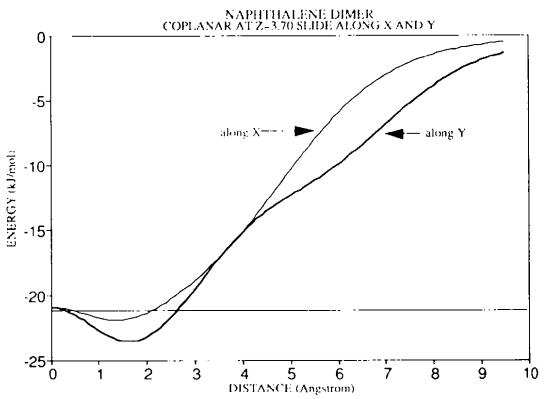

Fig. 4. Sliding model for coplanar naphthalene.

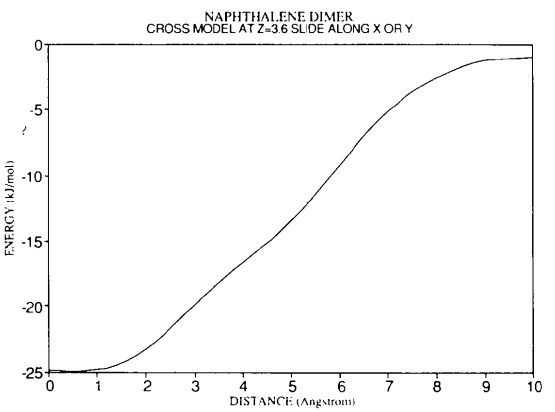

Fig. 5. Sliding model for crossed naphthalene.

model is even more suitable (Fig. 6). The coplanar model has an energy of -34.10 kJ mol^{-1} at a slightly reduced interplanar distance of 3.60 Å, compared to benzene or naphthalene. This is easily understood as a movement toward the graphite interlayer spacing of 3.34 Å where the ratio of C to H atoms becomes infinite. Sliding the top molecule along either X or Y decreases the energy (Fig. 7). The most favorable model is again the crossed orientation, which has

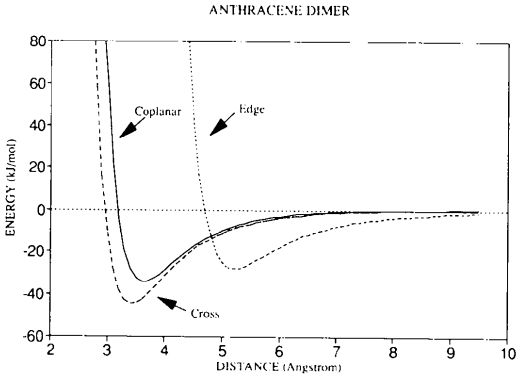

Fig. 6. Coplanar and edge models for anthracene.

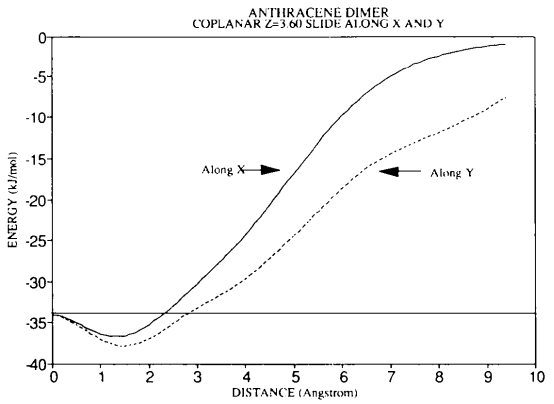

Fig. 7. Sliding model for anthracene.

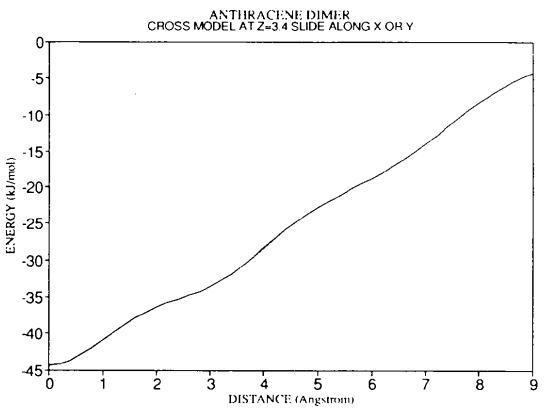

Fig. 8. Cross model for anthracene.

Table 4. *Benzene dimers extracted from the crystal compared to optimized gas dimer*

Symmetry operation	Distance (Å)	vdW (kJ mol^{-1})	COUL (kJ mol^{-1})	E (kJ mol^{-1})
2_1 along c	4.98	−6.43	−2.70	−9.14
2_1 along b	5.76	−5.10	−1.50	−6.59
2_1 along a	5.96	−4.06	−0.51	−4.57
(Gas dimer)	4.69	−10.38	−0.52	−10.90
*		−31.18	−9.42	−40.60
(Crystal)		−40.21	−11.37	−51.58

* Energy of reference molecule surrounded by 12 neighbors.

energy -44.34 kJ mol^{-1} at distance 3.40 Å. The cross model (Fig. 8) is not lowered in energy by a slide and this can be understood by considering the favorable orientation of the positively charged 9, 10 H atoms over negative carbon areas below. The edge model, as with naphthalene, is less favorable, with an energy of -28.01 kJ mol^{-1} at a distance of 5.2 Å.

Comparison to dimer interactions in the crystal

In order to compare gas dimer structures to molecular interactions in the crystal, pairs of nearby molecules in the crystals were extracted. The structure and energy of a molecular dimer abstracted from its crystal is not expected to be optimum for the isolated gas dimer. The presence of several nearest-neighbor molecules and of long-range intermolecular energy leads one to anticipate that these dimers will be different from optimum gas dimers, perhaps even radically. In crystals, nearest-neighbor interactions occur between molecules related either by lattice translations, space-group symmetry operations or a combination of these.

Benzene crystallizes in space group *Pbca* with four molecules in the cell positioned on inversion centers. Nearest-neighbor molecules are related by 2_1 screw axes along all three lattice directions. Table 4 shows intermolecular energies of benzene dimers extracted from the crystal. In benzene, close intermolecular interaction results from the three screw-axis symmetry operations. If we extract these three pairs of molecules from the crystal, keeping their relationship fixed, the calculated dimer intermolecular energies [using Williams & Starr (1977) nonbonded parameters] are -9.14 kJ mol^{-1} for the screw axis along c, -6.59 kJ mol^{-1} for the screw axis along b and -4.57 kJ mol^{-1} for the screw axis along a. Using the same force field, the predicted gas dimer structure has an energy of -10.90 kJ mol^{-1}. Thus it is seen that only one of the three nearest-neighbor interactions in the crystal is close to optimum energy for the gas dimer.

Fig. 9 shows a view of the benzene crystal structure perpendicular to a reference molecule placed at the origin. The 12 molecules surrounding the reference molecule are located at face centers of the cell; thus,

if the cell constants were cubic, the molecule centers would have f.c.c. packing. The space group places no restriction on the rotational orientation of the reference molecule, so there are six degrees of freedom for the crystal structure of rigid molecules (three molecular rotations and three cell constants). The 12 molecules are arranged in three groups of 4 corresponding to the three screw axes.

The four molecules related by the 2_1 axis along c are arranged in an edge model, with one above and one below the reference molecule and one to the left and one to the right. Fig. 10(a) shows this dimer extracted from the crystal. This edge model is modified, however, as compared to either the ideal edge orientation or the optimized gas dimer. In the ideal edge model, the distance is somewhat larger, 5.10 Å, and the energy is decreased to -10.06 kJ mol^{-1} (Table 3). In the optimized gas dimer, the distance is 4.69 Å and the energy is decreased to -10.90 kJ mol^{-1} (Table 4). The value of COUL in the symmetrical edge model, -2.36 kJ mol^{-1}, is similar to that for Fig. 10(a), -2.70 kJ mol^{-1}, but COUL in the optimized gas dimer is higher, -0.52 kJ mol^{-1}. The value of vdW in the symmetrical edge model, -7.70 kJ mol^{-1}, is intermediate between that for Fig. 10(a), -6.43 kJ mol^{-1}, and the optimized gas dimer, -10.38 kJ mol^{-1}. Molecule 10(a) has a closer center-to-center distance in the crystal (4.98 Å) than the symmetrical edge model (5.10 Å). The optimized gas dimer intermolecular distance is even smaller, 4.69 Å. Table 4 shows that molecule 10(a) is favored by a COUL value of -2.18 kJ mol^{-1} with a sacrifice of $+3.95$ kJ mol^{-1} in vdW, compared to the gas dimer. this is consistent with the long-range nature of COUL; in the crystal COUL becomes smaller (more favorable) and vdW becomes greater (less favorable).

The other two screw-axis interactions, shown in Figs. 10(b) and (c), have considerably higher energy. Both vdW and COUL are higher than those of 10(a). Clearly the crystal dimers in Figs. 10(b) and (c) are sacrificing both vdW and COUL to satisfy the packing requirements of 10(a) and the crystal as a whole. One must consider longer-range interactions, especially COUL, and the lattice-periodicity condition to understand why the latter two interactions are so unfavorable relative to the first interaction or to the gas dimers.

The last line of Table 4 shows that in this model COUL contributes 22% of the crystal energy of benzene. The fifth line of the table shows that 12 quasi-c.c.p. neighbors contribute -40.60 kJ mol^{-1}, *i.e.* 79% of the crystal energy. Within the quasi-c.c.p. shell COUL contributes 23%, which is nearly the same fraction for the crystal as a whole. Thus the partitioning of the energy between vdW and COUL is essentially already decided within the quasi-c.c.p. shell.

Both naphthalene and anthracene crystallize in space group $P2_1/c$ and there is only a single screw axis along b. Again, the molecules are placed on inversion centers. The packing of molecules is now a distorted h.c.p. structure instead of the distorted

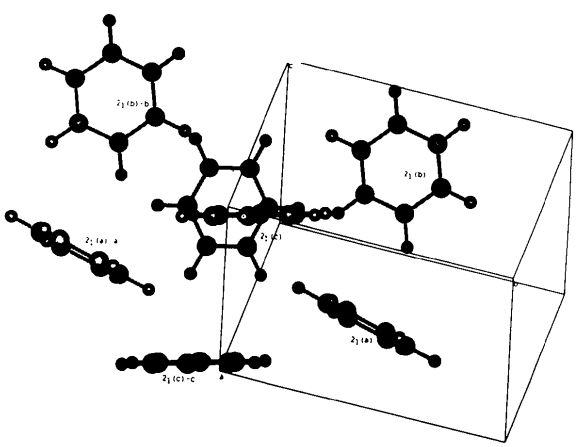

Fig. 9. Benzene quasi-c.c.p. type packing.

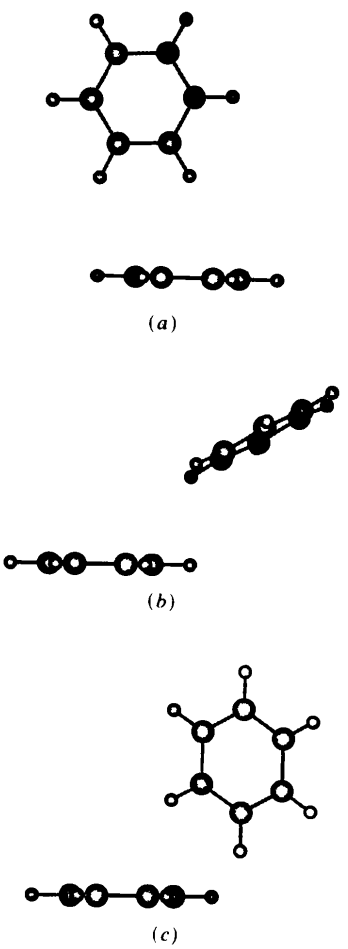

Fig. 10. Benzene dimers extracted from the observed crystal with symmetry (a) 2_1 along c; (b) 2_1 along b; (c) 2_1 along a.

c.c.p. structure of benzene (Fig. 11). The layers above and below are identical but translated by $c\cos\beta$ (−4.91 Å in naphthalene, −6.44 Å in anthracene) with interlayer distance $c\sin\beta$ (7.12 Å in naphthalene, 9.06 Å in anthracene). The figure shows that the long axis of the molecule is oriented predominantly perpendicular to the *ab* plane so that the interaction along *c* is largely edge-edge.

As compared to benzene, these crystal structures have distinct layers of molecules; intermolecular forces within a layer are stronger than those between layers. The first two entries of Table 5 show interactions within the *ab* layer plane of naphthalene. There are four interactions using the 2_1 along *b* and two interactions with the lattice translation *b*, making an approximately hexagonal layer pattern. Line 6 of the table shows that these six neighbors contribute −50.57 kJ mol^{-1}, *i.e.* 78% of the quasi-h.c.p. cluster energy. Line 7 shows that all 12 quasi-h.c.p. neighbors contribute −65.03 kJ mol^{-1}; thus, the interlayer energy within the quasi-h.c.p. cluster contributes only 22% compared to the expected 50% for an unlayered structure. All 12 of the quasi-h.c.p. neighbors contribute 83% of the crystal energy, which is close to the figure of 79% for quasi-c.c.p. neighbors in benzene. Note that the molecule related by *c* is not in the quasi-h.c.p. cluster; this interaction is included in the table because its energy is lower than one of the quasi-h.c.p. neighbors. The COUL contribution is greater within the layer: 20% as compared to 15% between layers. On the other hand, the vdW contribution is 80% within the layer and 85% between layers. Thus, the shape of the naphthalene molecule and its net atomic charges are such that COUL favors formation of a layered crystal structure. It is observed (Natkaniec, Belushkin, Dyck, Fuess, & Zeyen, 1983) that *ab* is a favored cleavage plane in the crystal.

Table 5. *Naphthalene dimers extracted from the crystal compared to optimized gas dimer*

Symmetry operation	Distance (Å)	vdW (kJ mol^{-1})	COUL (kJ mol^{-1})	*E* (kJ mol^{-1})
2_1 along *b*	5.02	−14.82	−2.74	−17.56
b	5.94	−10.75	−4.71	−15.45
2_1+c	7.76	−4.97	−0.93	−5.89
$a+c$	7.80	−2.34	−0.34	−2.68
c	8.648	−3.84	0.02	−3.82
*		−40.39	−10.19	−50.57
†		−52.67	−12.38	−65.03
(Crystal)		−66.54	−11.91	−78.45

* Energy of reference molecule surrounded by 6 neighbors in the *ac* plane.
† Energy of reference molecule surrounded by 12 neighbors.

Fig. 12(*a*) shows that the screw-axis interaction, which gives the lowest energy, is of edge-plane type.

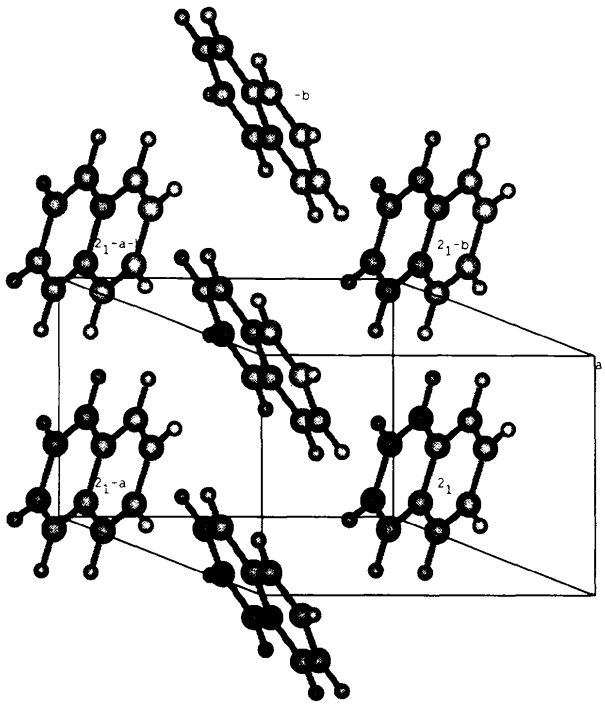

Fig. 11. Naphthalene quasi-h.c.p. packing.

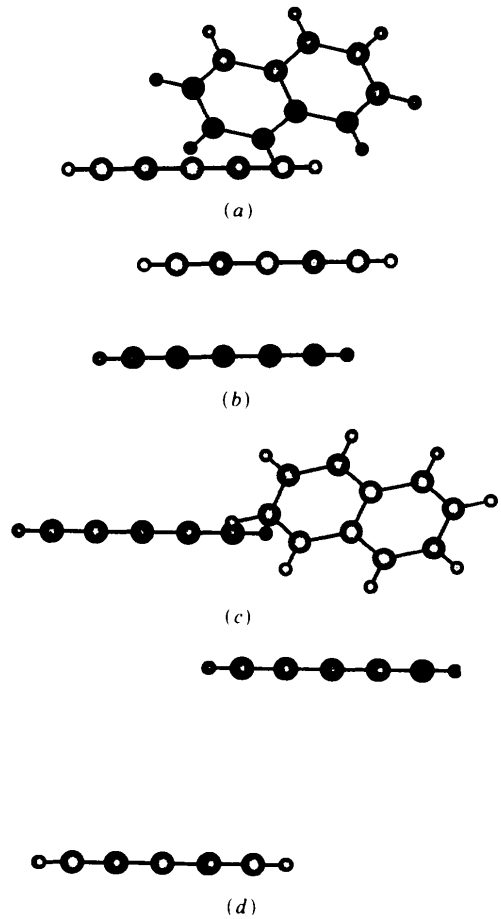

Fig. 12. Naphthalene dimers extracted from the observed crystal with symmetry (*a*) 2_1 along *b*; (*b*) *b* translation; (*c*) 2_1+c; (*d*) $a+c$.

Table 6. *Anthracene dimers extracted from the crystal compared to optimized gas dimer*

Symmetry operation	Distance (Å)	vdW (kJ mol^{-1})	COUL (kJ mol^{-1})	E (kJ mol^{-1})
2_1 along b	5.15	−22.62	−3.80	−26.42
b	6.00	−15.74	−7.80	−23.55
2_1+c	9.81	−5.80	−1.54	−7.33
$a+c$	9.27	−2.61	−0.41	−3.01
c	11.12	−3.67	−0.47	−3.19
*		−60.98	−15.4	−76.39
†		−75.19	−18.89	−94.06
(Crystal)		−91.82	−17.54	−109.36

* Energy of reference molecule surrounded by 6 neighbors in the *ac* plane.
† Energy of reference molecule surrounded by 12 neighbors.

It is interesting that the b translation (Fig. 12*b*), which is of coplanar-slide type, yields a strong interaction of −15.45 kJ mol^{-1}. Table 4 shows that this type of interaction can be optimized to an energy of −23.53 kJ mol^{-1} in the gas dimer. The 2_1+c and $a+c$ interactions (Figs. 12*c*, *d*) are both of edge-edge type and have higher energy.

The third and fourth entries of Table 5 show that the value of COUL between molecules in different layers is small (−0.93 and −0.34 kJ mol^{-1}), but note that the value of vdW also increases, especially for the $a+c$-related molecule. Since these edge-edge interactions contribute little COUL, it is not surprising that the crystal energy of naphthalene is only about 15% COUL compared with 20% for benzene. The extra interaction with a molecule along c shown as the fifth entry in Table 6 is outside the quasi-h.c.p. contribution. Yet this interaction is of lower energy than that of the molecule related by $a+c$, which is a quasi-h.c.p. neighbor.

The anthracene crystal (Fig. 13) shows a very similar pattern to naphthalene. The hexagonal six-coordination in the ab plane is again strong, as indicated by the first two lines in Table 6. The 2_1+c interaction, although at greater distance than the $a+c$ interaction, still has a lower energy of interaction (−7.33 *vs* −3.01 kJ mol^{-1}). As with naphthalene, the c interaction, although at a greater distance, has a favorable energy of −3.19 kJ mol^{-1}. Fig. 14 shows the quasi-h.c.p. dimers of anthracene.

The anthracene crystal energy is 16% COUL, which is comparable to naphthalene. The b dimer interaction energy in anthracene is stronger than in naphthalene, which is consistent with the slightly larger COUL. The six molecules within a layer contribute 81% of the quasi-h.c.p. cluster, which is slightly more than the corresponding figure of 78% for naphthalene. Thus, in anthracene only 19% of the quasi-h.c.p. cluster energy is of the interlayer type, compared to the expected 50% for a nonlayer structure. The quasi-h.c.p. cluster energy is 86% of the crystal energy, slightly larger the similar figure for naphthalene (83%).

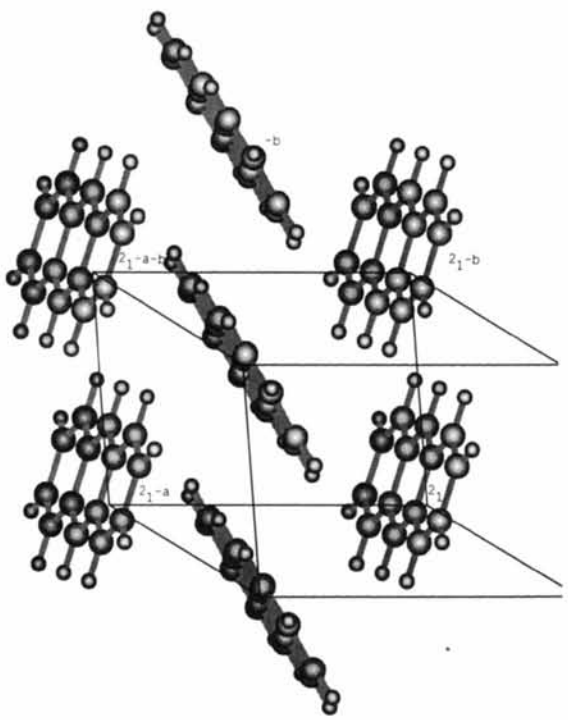

Fig. 13. Anthracene quasi-h.c.p. packing.

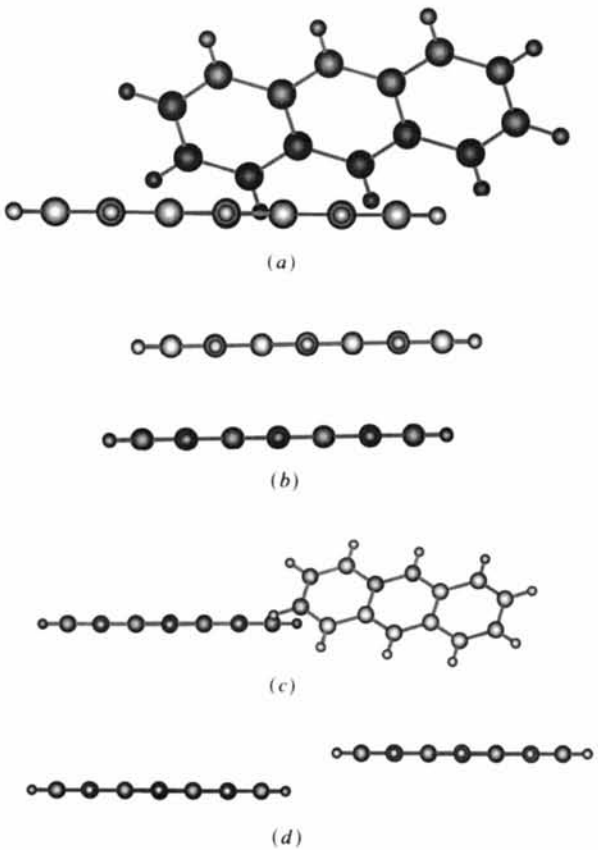

Fig. 14. Anthracene dimers extracted from the observed crystal. Symmetry identification as in Fig. 12.

Summary and concluding remarks

Three general types of intermolecular approach are distinguished for dimers of these flat aromatic molecules: coplanar with optional sliding motion, edge-to-plane and edge-to-edge. The presence of net atomic charges has a strong effect on both dimer and crystal structures. A coplanar approach allows the shortest distance between molecular centers and is favored by dispersion attraction as the molecular area increases. A sliding motion will lower the Coulombic energy of coplanar molecules. Edge-plane orientations are favored by electrostatic interaction between adjacent molecules and this orientation predominates in all three directions in the benzene crystal, where the molecules pack in quasi-c.c.p. fashion. However, naphthalene and anthracene utilize edge-plane interaction primarily only within quasi-h.c.p. layers. In these two structures, about 80% of the intermolecular energy originates within layers and only about 20% between layers.

References

BARTELL, L. S., HARSANYI, L. & VALENTE, E. J. (1989). *J. Phys. Chem.* **93**, 6201-6205.

BATTAGLIA, M. R., BUCKINGHAM, A. D. & WILLIAMS, J. H. (1981). *Chem. Phys. Lett.* **78**, 421-423.

BUCKINGHAM, A. D. & FOWLER, P. W. (1983). *J. Chem. Phys.* **79**, 6426-6428.

BUCKINGHAM, A. D. & FOWLER, P. W. (1985). *Can. J. Chem.* **63**, 2018-2025.

CARSKY, P., SELZLE, H. L. & SCHLAG, E. W. (1988). *Chem. Phys.* **125**, 165-170.

CHAPLOT, S. L., LEHNER, N. & PAWLEY, G. S. (1982). *Acta Cryst.* B**38**, 483-487.

COX, S. R. & WILLIAMS, D. E. (1981). *J. Comput. Chem.* **2**, 304-323.

FRISCH, M., BINKLEY, J. S., SCHLEGEL, H. B., RAGHAVACHARI, K., MELIUS, C. F., MARTIN, R. L., STEWART, J. J. P., BOBROWICZ, F. W., ROHLFING, C. M., KAHN, L. R., DEFREES, D. J., SEEGER, R. A., WHITESIDE, R. A., FOX, D. J., FLEUDER, E. M. & POPLE, J. A. (1988). *Program GAUSSIAN*86. Carnegie-Mellon Quantum Chemistry Publishing Unit, Pittsburgh, PA, USA.

GAVEZZOTTI, A. (1989). *J. Am. Chem. Soc.* **111**, 1835-1843.

HALL, D., STARR, T. H., WILLIAMS, D. E. & WOOD, M. K. (1980). *Acta Cryst.* A**36**, 494.

HALL, D. & WILLIAMS, D. E. (1975). *Acta Cryst.* A**31**, 56-58.

HURST, G. J. B., FOWLER, P. W., STONE, A. J. & BUCKINGHAM, A. D. (1986). *Int. J. Quant. Chem.* **29**, 1223-1239.

HWANG, J.-K. & WARSHEL, A. (1987). *Biochemistry*, **26**, 2669-2673.

KOLLMAN, P. & VAN GUNSTEREN, W. F. (1987). *Methods Enzymol.* **154**, 430-449.

LIU, S. & DYKSTRA, C. E. (1986). *Chem. Phys.* **107**, 343-349.

NATKANIEC, I., BELUSHKIN, A. V., DYCK, W., FUESS, H. & ZEYEN, C. M. E. (1983). *Z. Kristallogr.* **163**, 285-293.

POLITZER, P., LAURENCE, P. R. & JAYASURIYA, K. (1985). *Environ. Health Perspect.* **61**, 191-202.

PRICE, S. L. & STONE, A. J. (1987). *J. Chem. Phys.* **86**, 2859-2868.

SHI, X. & BARTELL, L. S. (1988). *J. Phys. Chem.* **92**, 5667-5673.

STEED, J. M., DIXON, T. A. & KLEMPERER, W. (1979). *J. Chem. Phys.* **70**, 4940-4946.

STERNLICHT, H. (1964). *J. Chem. Phys.* **40**, 1175-1188.

VALENTE, E. J. & BARTELL, L. S. (1984). *J. Chem. Phys.* **80**, 1451-1457.

VENANZI, C. A. & BUNCE, J. D. (1986). *Int. J. Quantum Chem. Quantum. Biol. Symp.* **12**, 69-87.

WAAL, B. W. VAN DE (1984). *Acta Cryst.* A**40**, 306-307.

WARSHEL, A. (1981). *Acc. Chem. Res.* **14**, 284-290.

WILLIAMS, D. E. (1974). *Acta Cryst.* A**30**, 71-77.

WILLIAMS, D. E. (1980). *Acta Cryst.* A**36**, 715-723.

WILLIAMS, D. E. (1988). *Program PDM*88. Quantum Chemistry Program Exchange, Indiana Univ., USA.

WILLIAMS, D. E. (1991*a*). *PCK*91. *A Crystal Molecular Packing Analysis Program.* Chemistry Department, Univ. of Louisville, USA.

WILLIAMS, D. E. (1991*b*). *Reviews in Computational Chemistry* II, edited by K. B. LIPKOWITZ & D. B. BOYD, pp. 219-271. New York: VCH Publishers.

WILLIAMS, D. E. & STARR, T. H. (1977). *J. Comput. Chem.* **1**, 173-177.

Acta Cryst. (1993). A**49**, 10-22

Internal Vibrations of a Molecule Consisting of Rigid Segments. I. Non-interacting Internal Vibrations

BY XIAO-MIN HE

ES76 Biophysics Branch, National Aeronautics and Space Administration, Space Science Laboratory, Marshall Space Flight Center, AL 35812, *USA*

AND B. M. CRAVEN

Department of Crystallography, University of Pittsburgh, Pittsburgh, PA 15260, *USA*

(*Received* 30 *September* 1991; *accepted* 11 *May* 1992)

Abstract

For molecular crystals, a procedure is proposed for interpreting experimentally determined atomic mean square anisotropic displacement parameters (ADPs) in terms of the overall molecular vibration together with internal vibrations with the assumption that the molecule consists of a set of linked rigid segments.

0108-7673/93/010010-13$06.00